An Experimental Study on the Transient Interaction Between High Temperature Thermite Melt and Concrete

Ki-Man Nho

Korea Electric Power Research Institute

P.O. Box 103, Yusong, Taejon 305-380, Korea

Jong-Hwan Kim, Sang Baik Kim

Korea Atomic Energy Research Institute

150 Dukjin-dong, Yusong-gu, Taejon 305-353, Korea

Ki-Yeol Shin and Mo Chung

Yeungnam University

School of Mechanical Engineering

214-1 Dae-dong, Kyongsan 712-749, Korea

Abstract

During postulated severe accidents in Light Water Reactors, molten corium, which was ejected from the reactor vessel bottom, may erode the concrete basemat of the containment and there by threaten the containment integrity. This study experimentally examines the molten core-concrete interaction (MCCI) using 20kg of thermite melt ($Fe + Al_2O_3$) and the concrete, used in Yonggwang Nuclear Power Plant Units 3 and 4 (YGN 3 & 4) in Korea. The measured data are the downward heat fluxes, concrete erosion rate, gases and particle generation rates during MCCI. Transient results were compared with those of TURC1T experiment conducted by SNL in USA. The peak downward heat flux to the concrete was measured to be about $2.1MW/m^2$. The initial concrete erosion rate was 175cm per hour, decreasing to 30cm per hour. It was shown from the post-test that the erosion was progressed downward up to 18mm in the concrete slug.

1. Introduction

During severe core meltdown accidents in the Light Water Reactors, high temperature (about 3000K) molten corium may be ejected from the pressurized reactor vessel bottom. When it interacts with the concrete basemat of the reactor cavity, combustible gases (H_2, CO) and fission products would be released. By the pressurization and/or the combustion of the gases, the containment integrity could be threatened. Unless sufficient cooling such as overlying water injection is provided, the coolability of the melt may not be guaranteed.

Since the TMI accident in 1979, the interaction of

the core melt with the concrete basemat has drawn interests in the study of concrete erosion, generations of steam, non-condensable gases and aerosols. The interaction is usually associated with the high temperature heat transfer at three different layers of overlying water, melt and concrete under gas environment. The understanding of overall heat transfer characteristics is crucial for the design of the next generation containment, which will have enough basemat thickness and melt spreading area to cool the corium effectively.

Various experimental and theoretical studies have been conducted in USA and Germany to develop an integral computer code, which will be used to determine the overall molten core coolability. Since mid 80s, Sandia National Laboratories[1, 2, 3, 4, 5] in USA and FZK[6] in Germany have conducted a series of MCCI experiments to measure the concrete erosion rate, gas generation and heat fluxes. They used local concretes such as basaltic (BAS) and/or limestone common sand (LCS) as basemat material and SUS304, Mild steel, UO_2-ZrO_2-Zr and Fe+Al_2O_3 as corium simulant. The main objectives of the MCCI experiments so far were to improve MCCI codes such as WECHSL[6], CORCON[7] and VANESA[8]. Recently, Argonne National Laboratory in USA is conducting ACE[9,10] and MACE[11,12] experiments. They have conducted experiments to study the heat transfer characteristics of the melt quenched by overlying water on the corium simulant. It is known that most computer codes for MCCI such as WECHSL[6], CORCON[7] and VANESA[8], contain considerable uncertainties and are still being updated based on recent experimental data. To study Korean concrete behavior accurately, it is necessary to know the property data of local concrete in Korea. The experiments will provide data for the physical processes involving the high-temperature heat transfer and production of combustible gases, aerosol and fission products, which are generated from the molten debris of the local concrete in Korea. The other objective of this study is to understand the characteristics of

local concrete in YGN 3 & 4, Korea by conducting experiments using transient thermite heating without overlying water injection. The experimental results have been compared with those of TURC1T experiment where thermite melt was used as a melt simulant. This study consists of two MCCI Experiments, MEK0 and MEK1. The MEK0 test was performed in an open space while the MEK1 test in a large aluminum alloy protection vessel. In the experiments, 20 kg of thermite melt was poured on the actual concrete used in YGN 3 & 4, Korea. Parameters such as concrete erosion rate, downward and sideward heat flux were measured in both experiments.

2. Experimental Procedure

The experiment focuses on the transient, one-dimensional, downward concrete erosion without overlying water injection and Fe+Al_2O_3 thermite is used as a melt simulant. The experimental program consists of two tests ; MEK0 and MEK1 tests. MEK0 test was performed in an open space to confirm the integrity
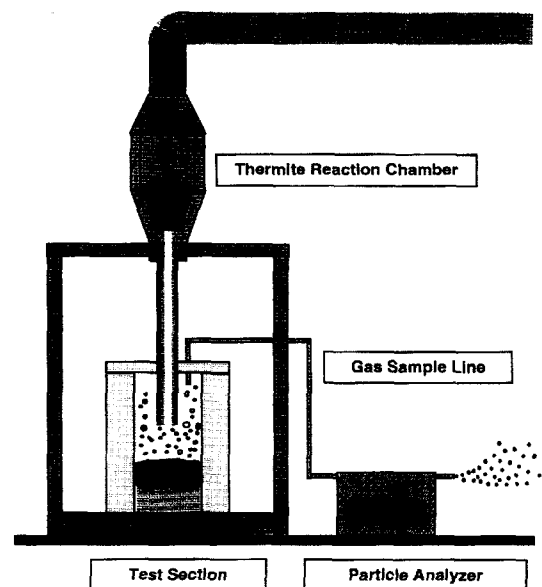

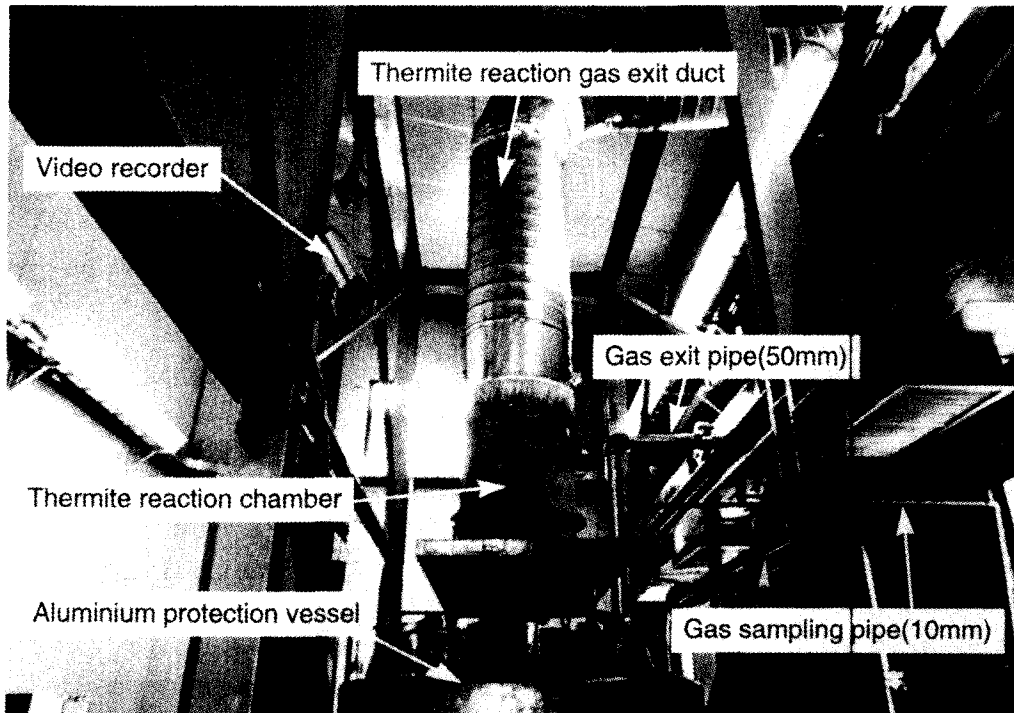Fig. 1. Schematic Diagram of Experimental Apparatus.

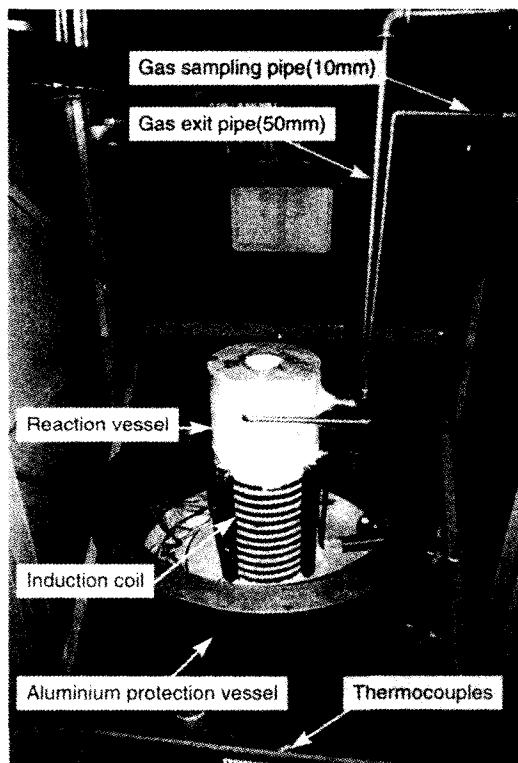Fig. 2.(a) Photograph of Experimental Facility for MEK1 Test; Melt Generator.

Fig. 2.(b) Photograph of Experimental Facility for MEK1 Test; Reaction Vessel.

of reaction vessel, melt transport channel and instrumentation while MEK1 test in a large aluminum alloy vessel inside the laboratory. The vessel has a diameter of 1.24m and a height of 1.5m.

The experimental facility is shown schematically in Figure 1 and the photograph of the assembled apparatus in Figure 2. The facility consists of two major components; the melt generator where the melts are produced and the reaction vessel. The melt generator consists of a thermite reaction chamber and a transport channel as shown in Figure 2(a). The thermite reaction chamber was made of stainless steel with a 50mm thick alumina insulation inside. The reaction chamber can contain maximum 40kg of thermite and has a diameter of 400mm, a height of 450mm and a thickness of 5mm. The bottom part of the chamber has a conical shape for easy melt drain. The melt transport channel was made of alumina powder with a stainless steel liner, having inner diameter of 120mm, length of 1200mm and 30mm thick alumina insulation inside. Once the thermite is ignited by the AC 24 Volts electricity, aluminum and iron
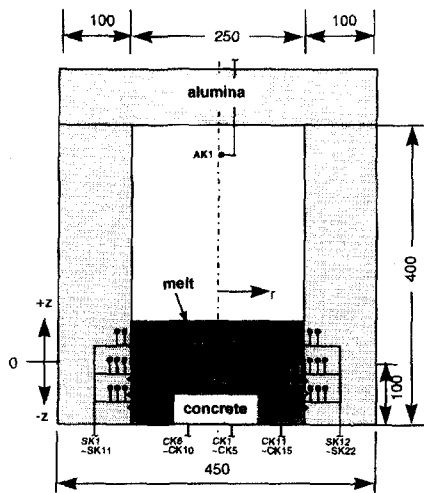
(a) MEKO Test Cylinder
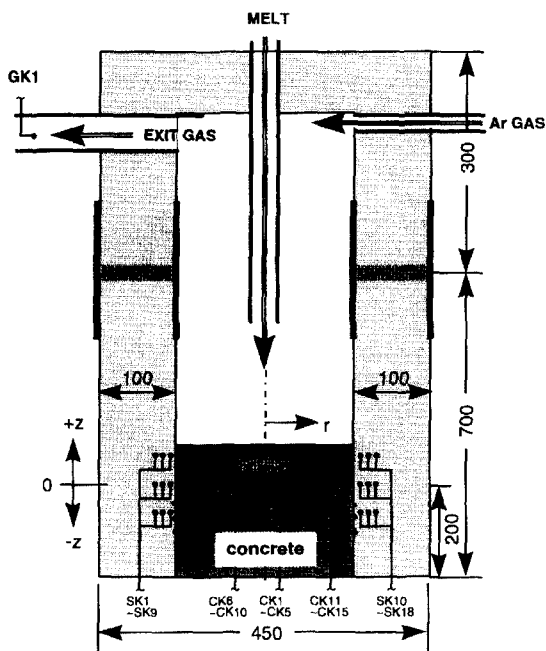
(b) MEK1 Test Cylinder

Fig. 3. Locations of Thermocouples within Reaction Vessel.

oxide (Fe_2O_3) powders starts to react each other chemically, yielding a high temperature above $2400 \pm 50\,^{\circ}C$ [2]. This temperature can melt the thin

Table 1. Engineering Composition of Concrete in YGN 3&4.

Item	Proportion	Fraction
Water	285LB	7.6%
Cement, type V	678 LB	18.1%
Sand	1275 LB	34.1%
Aggregate, 19mm	1505 LB	40.2%
Total	3743 LB	100.0%
Water Reducing Agent	923ml	
Air Entraining Agent	16ml	
Compression Strength	5500 PSI	

plug, which was installed at the bottom of the reaction chamber, allowing thermite melts to drop onto the concrete specimen through the transport channel to start MCCI soon.

The interaction crucible, shown schematically in Figure 3, consists of a test concrete slug and Alumina annulus. The interaction crucible was fabricated in two major steps; the construction of the Alumina annulus and the casting of the concrete slug. The annular reaction vessel was constructed using "MINRO-AL CAST A44" Alumina of 95.5% purity, Grain size 14 Mesh (1.4mm), manufactured by Allied Mineral Products in USA. The reaction vessels for both tests have different heights of 400 mm for MEKO test and 700mm for MEK1 test respectively, to provide more space for gas generation. The side and bottom wall thicknesses were 100mm and inner diameters were 250mm for MEKO test and 240mm for MEK1 test, respectively. After casting, the Alumina annular vessels were cured at ambient air temperature for three days(72hours). Further curing was accomplished by using a heating element inside the vessel keeping the temperature at about 200°C for 24 hours. In the side wall of the Alumina reaction vessel, K-type thermocouples were installed to measure the heat flux to the side wall. A total of 22 K-type thermocouples were embedded in MEKO test crucible and 18 thermocouples in MEK1 test crucible, respectively.

Table 1 summarizes the engineering composition

of the local concrete in YGN 3 & 4, Korea. It was poured into the reaction vessel to have thicknesses of 100mm for MEK0 test and 200mm for MEK1 test, respectively. Once a homogeneous mixture was achieved, two test cylinders were cast. The concrete was allowed to cure for a minimum of 90 days before tests to meet the specification suggested by the American Concrete Institution. Curing was performed at ambient conditions. Considering expected temperature range for the concrete, which is below 1200℃, a total of 15 K-type thermocouples (Chromega versus Alomega) with the sheath diameter of 1. 6mm (AWG Gage number 30) were embedded in the concrete specimen to measure the heat flux and the erosion rate. Figure 3 shows locations of the thermocouples. Three bundles of 5 thermocouples were placed at different radial locations, 5mm apart below the concrete surface. One OMEGA C-type thermocouple (Tungsten 5% Rhenium versus Tungsten 26% Rhenium) with sheath diameter of 1.6mm was installed 20mm above the concrete surface to measure the melt temperature. It was insulated with 10mm thick Magnesia (MgO) to protect from the possible damage by the high temperature thermite melt.

The temperature data signals were transmitted to FLUKE NetDAQs data acquisition system (DAS) and were processed by the personal computer. This system has a data collection rate of 20 to 1000 samples per a second and an accuracy of 0.6℃. Data acquisition program on the PC was directly displayed in the Excel spreadsheet using the Dynamic Data Exchange (DDE) function. Five gas sampling bottles and on-line 10 stage cascade impactors with cyclones, manufactured by ITP, USA were connected to the gas exit from the top of the reaction vessel. For the instantaneous aerosol analysis, On-line 10 stage particle analyzer, made by California Measurements Inc., USA, was used in parallel. A constant flow rate of argon gas was supplied through the top of reaction vessel to dilute combustible gases and to carry the gases generated during the MCCI. The collected gases sampled at different intervals during the experiment were analyzed after the experiment with Hewlett Packard 5890 Gas Chromatograph.

3. Analysis of Experimental Data

In our study, the concrete erosion rate and heat flux were calculated at the boundary surface between molten pool and concrete using measured temperature data. The concrete erosion rate was estimated by detecting thermocouples failures attacked by the molten melt, which were noticed by the steep rise in measured temperatures. It was noticed that the K-type thermocouples with a sheath diameter of 1.6mm were failed at the temperature of 1372℃.

The ablation temperature of the concrete are different with the concrete type. Since it has not been measured yet for the Korean concrete, the value from the CORCON MOD 3 will be used. The downward heat flux varies with the concrete erosion rate during the erosion and depends on the amount of heat conduction to the concrete after the erosion. By eliminating the ablative concrete side wall, reaction products generated at the core debris-concrete interaction can be quantified, without the influence of reaction products generated for different thermophysical conditions at the side walls. The crucible design has been labeled as a one-dimensional crucible. Assuming a quasi-steady state erosion, a moving boundary model can be used to calculate heat transfer rate[13]. Figure 4 shows a control volume located between s- and v-surfaces. One-dimensional energy equation at the erosion front (u-surface) surrounded by neighboring surfaces (s, v) is

$$
\begin{aligned}
q_s &= \dot{G}(h_s - h_v) + q_v \\
&= \dot{G}(h_{fs} + h_u - h_v) + q_v \\
&= \dot{G}(h_{fs} + c_p(T_u - T_v)) + q_v
\end{aligned} \tag{1}
$$

where q_s is the heat flux at the boundary s-surface, $\dot{G}$ is the mass flux during erosion, h_s, h_u, h_v are the enthalpies at the surfaces s, u and v, respectively, h_{fs} is the latent heat of fusion of the concrete, c_p is the specific
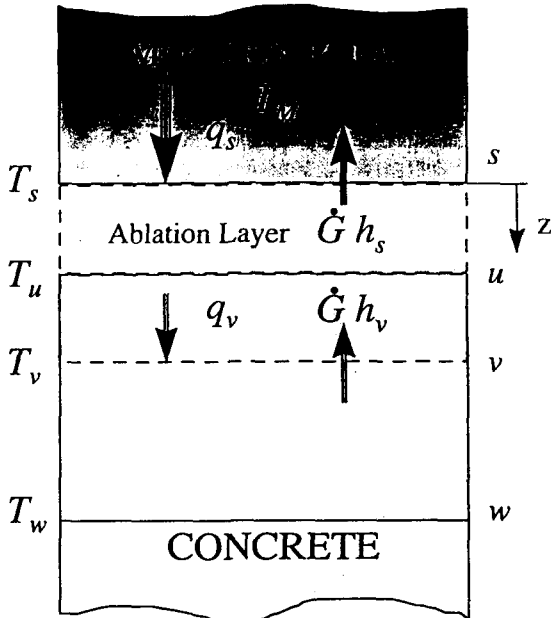
Fig. 4. Control Volume for One-dimensional, Steady-state Ablation.

heat of the concrete, and q_v is the heat flux at the surface v. The mass flux can be calculated from the fact that the product of concrete density, erosion rate, dz/dt, and enthalpy difference between s and u surfaces equal to the latent heat of fusion for the concrete. Assuming that the temperature at the eros-

ion front, T_u is equal to the concrete ablation temperature, T_{ab}, the heat flux at the boundary s-surface is given by

$$q_s = \rho \frac{dz}{dt}\bigg|_{s-v} (h_{fs} + c_p(T_{ab} - T_v)) + q_v \quad (2)$$

when the erosion stops at the surface v, the erosion rate becomes zero and then conduction plays the main role in heat transfer to the concrete. The amount of conduction heat transfer becomes

$$q_s = q_v = -k\frac{dT}{dz}\bigg|_{v-w} \quad (3)$$

where k is the thermal conductivity of the concrete. Assuming that the material properties of the Korean concrete are similar to those of US basaltic (BAS) concrete, thermal properties in Table 2[2, 5, 7, 14] were used in the analysis. The chemical composition of the local concrete in YGN 3 & 4 measured by the Ssangyong Concrete Research Center in Taejon, Korea was used in the analysis. A summary of the chemical composition of the concrete is shown in Table 3 [7, 14, 15].

4. Results and Discussion

Two MCCI experiments have been carried out in

Table 2. Thermal Properties of Concretes Mostly used in NPP Basemat.

Concrete type Property	Basaltic	Limestone common sand	Limestone	This study
Density $\rho(kg/m^3)$	2340	2340	2340	2400
Solidus temperature T_S (K)	1350	1420	1690	1350
Ablation temperature T_{ab} (K)	1450	1500	1750	1450
Liquidus temperature T_L (K)	1650	1670	1875	1650
Latent heat of fusion h_{fs} (J/kg)	0.5~0.6E6	0.56E6	0.5~0.9E6	0.5E6
Thermal conductivity k (W/mK)		$-0.0012T+2.4$		$-0.0012T+2.4$

Table 3. Chemical Composition of Concretes Mostly used in NPP Basemat(weight %)

Composition \ Concrete type	Basaltic	Limestone common sand	Limestone	YGN 3 & 4
SiO_2	54.84	35.80	3.60	54.90
CaO	8.82	31.30	45.40	16.90
Al_2O_3	8.32	3.60	1.60	11.80
K_2O	5.39	1.22	0.68	2.44
Na_2O	1.80	0.082	0.078	1.39
$MgO + MnO + TiO_2$	7.21	0.69	5.80	2.50
Fe_2O_3	6.26	1.44	1.20	4.10
Cr_2O_3	0.00	0.014	0.004	0.02
H_2O	5.86	4.70	5.94	3.00
CO_2	1.50	21.154	35.698	3.00
Total	100	100	100	100.05

this study. The objectives of the MEK0 test, which was conducted outside the laboratory for safety reason, were to measure local concrete erosion rate and downward heat flux and hence to evaluate the integrity of the crucible and melt transport channel during
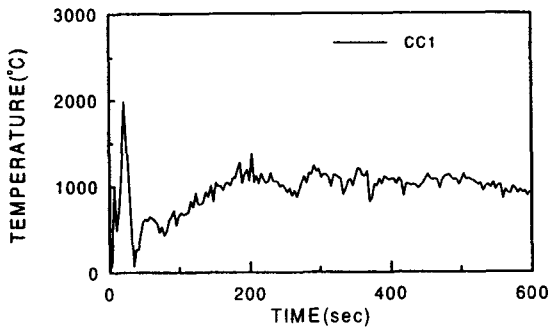
Fig. 5. Molten Thermite Temperature Measured During MEK0 Test.
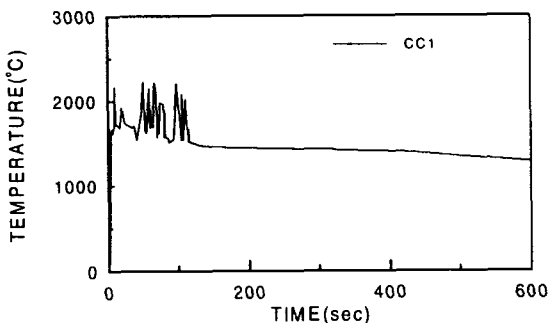
Fig. 6. Molten Thermite Temperature Measured During MEK1 Test.

the thermite reaction. MEK1 test was performed inside the laboratory using the large aluminum alloy protection vessel to simulate one-dimensional MCCI phenomenon and to evaluate the integrity of protection vessel for future sustained heating experiments.

Figures 5 and 6 show the temperature history of the thermite melt during MCCI. In spite of the MgO insulation outside, the C-type thermocouple located at CC1 in Figure 3 was failed due to a rapid temperature rise as it comes into contact with the melt. The peak melt temperature was measured to be 1985℃ in MEK0 test and 2230℃ in MEK1 test, respectively, The initial melt temperature was reported to be about 2247℃ in TURC1T test[2]. The higher melt temperature in the MEK1 test is due to better insulation by the protection vessel.

Figures 7 to 12 show the concrete temperature history at 0, 5, 10, 15, 20mm below the concrete surface (Figures 7 to 9 for MEK0 Test and Figures 10 to 12 for MEK1 Test) while Figure 3 shows locations of thermocouples for MEK0 and MEK1 Tests.

After the experiment, the reaction vessel was cut through axially to observe the concrete erosion front. Figure 13 (a) shows the cross section of the reaction vessel. A 2~3mm thick crevice was observed between the solidified melt and the erosion front. The debris generated during MCCI were also observed. As seen in Figure 13 (b), the erosion front was found
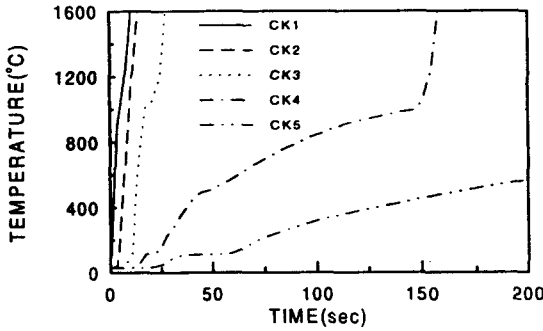
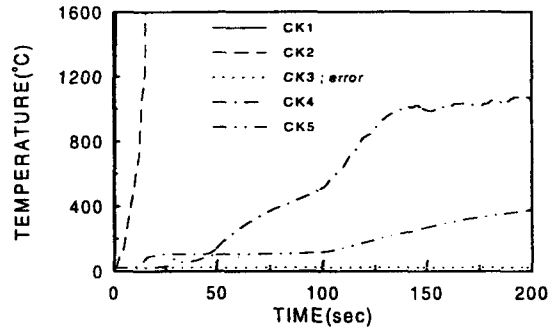Fig. 7. Concrete Temperature at r=0mm (Center) in MEK0 Test.

Fig. 10. Concrete Temperature at r=0mm (Center) in MEK1 Test.
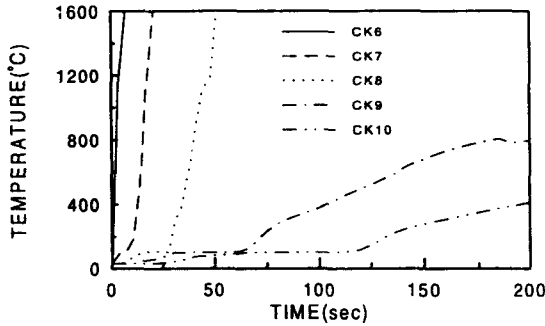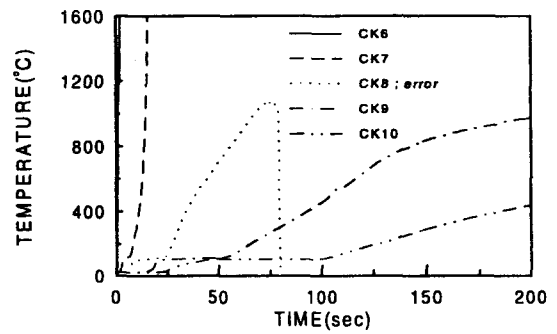

Fig. 8. Concrete Temperature at r=62.5mm in MEK0 Test.

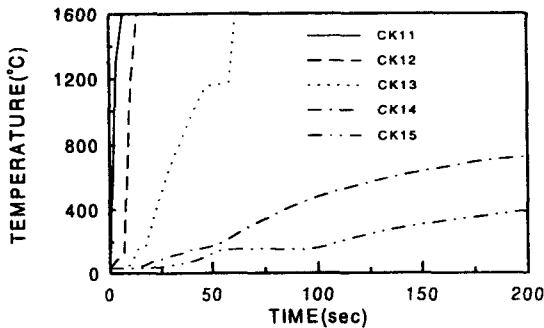
Fig. 11. Concrete Temperature at r=62.5mm in MEK1 Test.
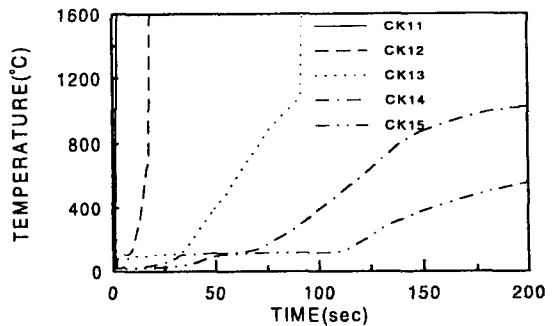

Fig. 9. Concrete Temperature at r=105mm for MEK0 Test.

Fig. 12. Concrete Temperature at r=105mm in MEK1 Test.

to be radially irregular and bow-shaped. The maximum erosion depth was measured to be about 18mm.

Figure 14 shows the concrete ablation front as a function of time assuming the erosion temperature of the concrete is 1177°C. The maximum erosion rate was found to be 129cm per hour for MEK0 test and 175cm per hour for MEK1 test at the start of concrete erosion, decreasing to 30cm per hour at the end of both tests. When compared with TURC1T[2] experiment where 200kg of thermite was used as melt simulant, the measured concrete erosion rates
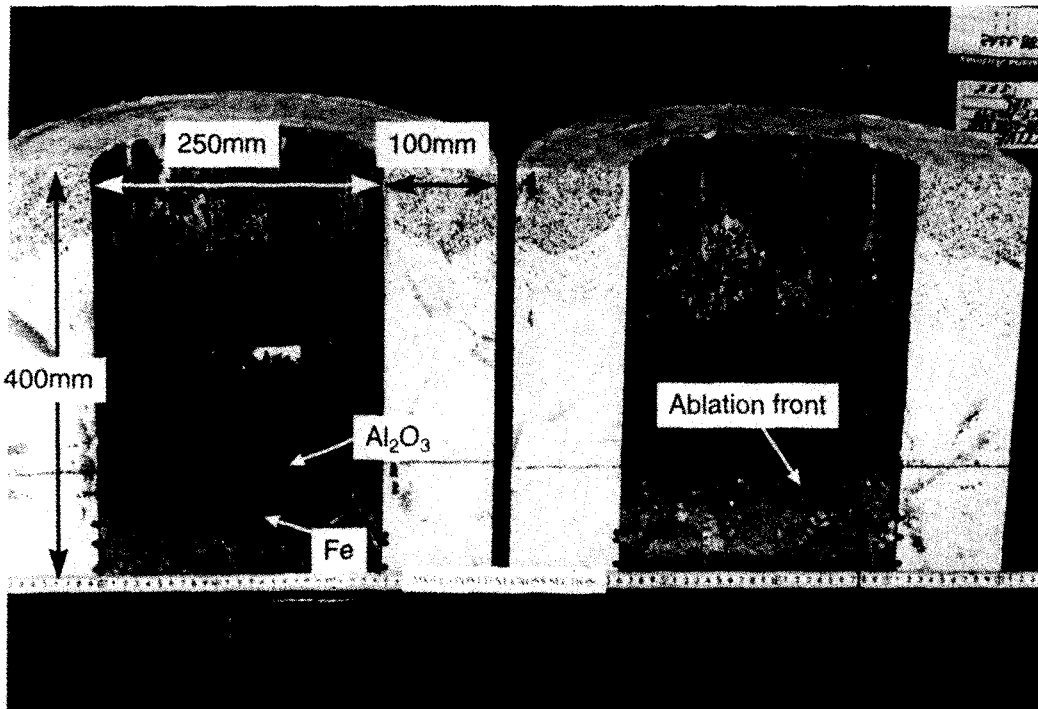
(a) Cross Sectional View
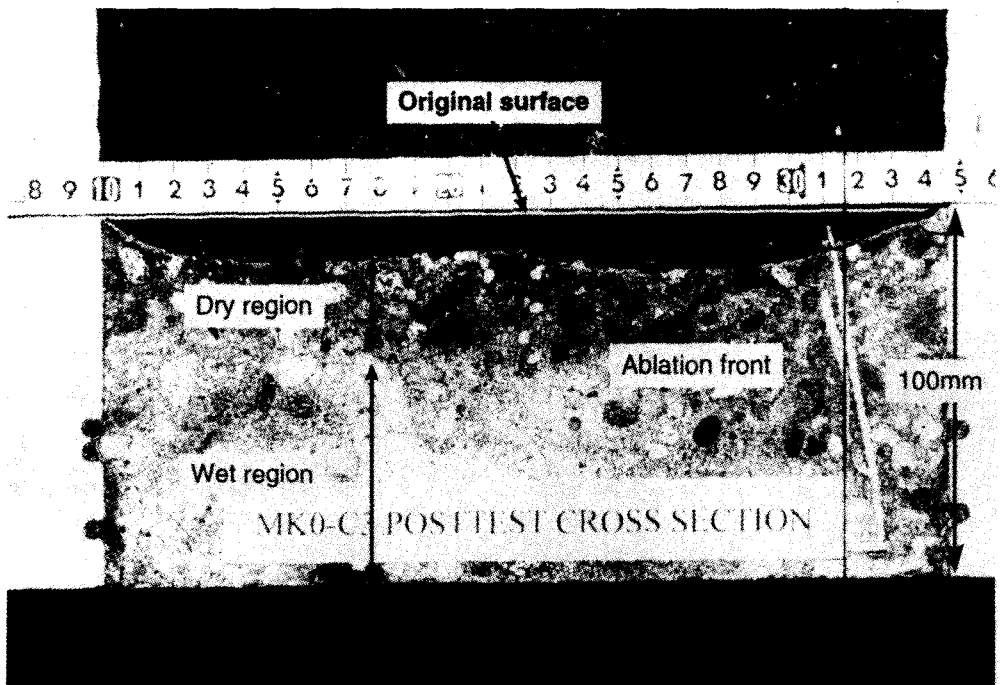
(b) Ablation Front

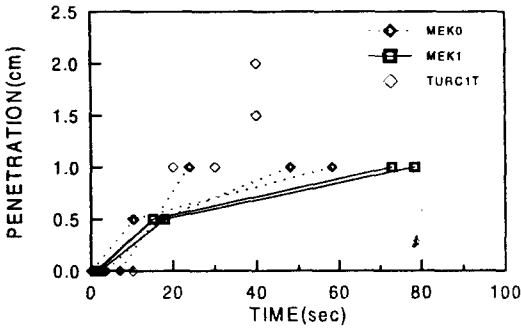Fig. 13 Photograph of the Post-MEK0 Test Cylinder.

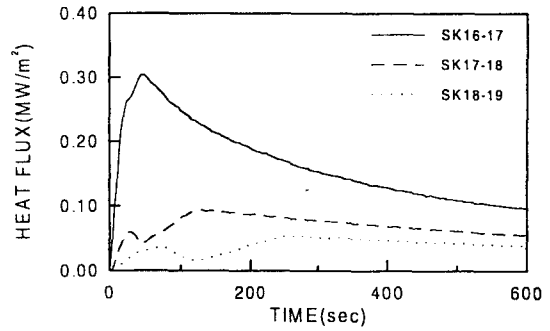Fig. 14. Concrete Ablation Front in MEK0 and MEK1 Tests.
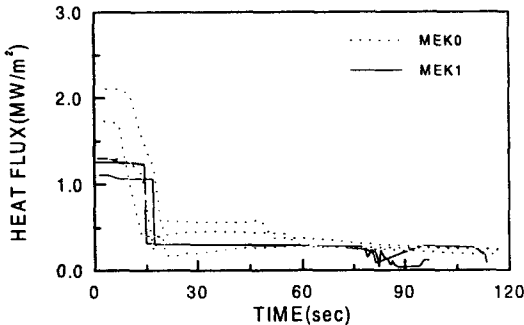

Fig. 15. Heat Flux to the Concrete in MEK0 and MEK1 Tests.

Fig. 16. Temperature History of the Side Wall at z=0mm in MEK0 Test.

Fig. 17. Heat Flux to the Alumina Crucible at z=0mm in MEK0 Test.

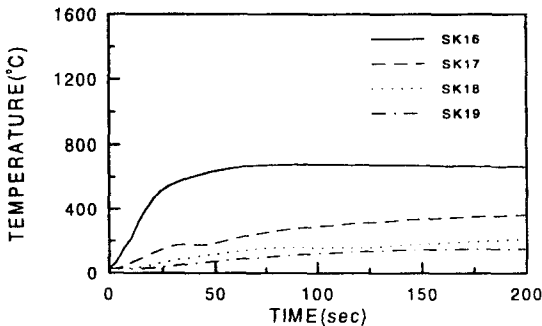
Fig. 18. Temperature History of the Exit Gas in MEK1 Test.

in both MEK0 and MEK1 tests are in the close range (2cm at 40 seconds in TURC1T test[2] versus 1cm at 20 seconds in MEK0 test). It can be concluded that the concrete erosion rate seems to be more influenced by the melt temperature than the melt mass. Figure 15 shows the measured heat flux to the concrete with the maximum value of about 1.1~2. 1MW/m² at the start of concrete erosion. For the transient test with thermite heating, the heat flux to the concrete was decreased quickly (within 15 seconds) after the initial contact with the concrete, as seen in Figure 15.

Figure 16 shows the temperature history of the alumina crucible while Figure 17 presents the heat flux to the side wall. The location of SK16 thermocouple is close to the inner wall and SK19 close to the outer wall. The maximum value of 0.3MW/m², which is much less than the value for the bottom concrete (1.1~2.1 MW/m² at the start of concrete erosion), was measured. It was observed that the side wall heat flux is about 1/4 to 1/7 of the downward heat flux at the start of the erosion. The gas tem-

perature measured at the gas exit from the reaction vessel rose rapidly to 650℃ during the first 15 seconds after the melt ejection, decreasing to 200℃ after 300 seconds as shown in Figure 18. During our experiments, sampling of gases and aerosol particles started 660 seconds after the melt ejection. Since thermite melt temperature was close to the concrete ablation temperature, the amount of individual gases such as H_2, CO and CO_2 were not recorded, but only a small amount of CO_2 gas was measured.

5. Conclusions

MCCI experiment was performed using 20kg thermite melt on the local Yonggwang concrete in Korea. Experiments showed that the erosion depth, rate of erosion and heat flux were highly dependent on the initial melt temperature. Other important findings are

1) The peak melt temperature was measured to be 2230℃ by the C-type thermocouple.
2) The maximum concrete erosion depth was measured to be about 18mm and the erosion rate steadily decreased from 129~175cm per hour to 30cm per hour towards the end of interaction during the experiments.
3) The peak downward heat flux was measured to be 1.1~2.1 MW/m^2 at the start of the concrete erosion.

Nomenclature

c_p	specific heat at constant pressure, J/kgK
h	enthalpy, J/kg
h_{fs}	latent heat of fusion, J/kg
k	thermal conductivity, W/mK
G	mass flux, kg/m^2s
q	heat flux, W/m^2
t	time, s
T	temperature, K
T_{ab}	concrete ablation temperature, K
z	coordinate, m

Subscripts

L	liquid phase
S	solid phase
s,u,v,w	control volume surfaces

Greek Symbols

ρ	density, kg/m^3

References

1. E.R. Copus, and D.R. Bradley, "Interaction of Hot Solid Debris with Concrete," *NUREG/CR-4 558*, SAND85-1739, R5, R7(1986).
2. J. E. Gronager, A.J. Suo-Antilla, D.R. Bradley, and J.E. Brockmann, "TURC1 : Large Scale Metallic Melt-Concrete Interaction Experiments and Analysis," *NUREG/CR-4420*, SAND85-0707 R5, R7(1986) and "TURC2 and 3 : Large-Scale UO2/ZrO2/Zr Melt-Concrete Interaction Experiments and Analysis," NUREG/CR-4521, SAND 86-0318 R5, R7(1986).
3. W.W. Tarbell, D.R. Bradley, R.E. Blose, J.W. Ross, and D.W. Gilbert, "Sustained Concrete Attack by Low-Temperature Fragmented Core Debris," NUREG/CR 3024, SAND82-2476 R3, R4 (1987).
4. R.E. Blose, J.E. Gronager, A.J. Suo-Anttilla, and J.E. Brockmann, "SWISS : Sustained Heated Metallic Melt/Concrete Interactions with Overlying Water Pools," *NUREG/CR4727*, SANDS85-1546 R3, R4, R7(1987).
5. D.E. Bradly, and E.R. Copus, "Significant Results from SURC-3 and SURC-3A Experiments," *15th Water Reactor Safety Meeting*, National Bureau of Standards, Gaithersburg(1987) and E. R. Copus et al., "Core-Concrete Interactions Using Molten Steel with Zirconium on a Basaltic Basemat : The SURC-4 Experiment," *NUREG/CR-4994*, SAND87 -2008, R3, R4, R7(1987) and M. Lee, and R.A. Bari, "SURC-4 Experiment on

Core-Concrete Interactions," *OECD/NEA*, CSNI Report, No. 155, Vol. 2(1988).

6. H. Alsmeyer, "BETA Experiments in Verification of the WECHSL Code : Experimental Results on the Melt-Concrete Interaction," *Nuclear Engineering and Design*, Vol. 103, pp. 115~125 (1987) and H. Alsmeyer et al., "BETA Experimental Results on Melt/Concrete Interactions : Silicate Concrete Behavior," Proc. of the *Committee on the Safety of Nuclear Installations (CSNI) Specialists Meeting on Core Debris-Concrete Interactions*, EPRI, NP-5054-SR(1987).

7. D.E. Bradley et al., "CORCON-MOD3 : An Integrated Computer Model for Analysis of Molten Core-Concrete Interactions," *User's Manual*, NUREG/CR-5843, SAND92-0167(1993).

8. D.A. Power et al., "VANESA : A Mechanistic Model of Radionuclide Release and Aerosol Generation During Core Debris Interactions with Concrete," *NUREG/CR-4308*, SAND85-1370 (1986).

9. D.H. Thompson et al., "Thermal-Hydraulic Aspects of the Large Scale Integral MCCI Tests in the ACE Program," *Proc. of the 2nd OECD*

(NEA) CSNI Specialist Meeting on Molten Core Debris-Concrete Interaction, KfK 5108, NEA/CSNI/R, pp. 97~110(1992).

10. J.K. Fink et al., "Aerosol and Melt Chemistry in the ACE Molten Core-Concrete Interaction Experiments," *High Temperature and Materials Science*, Vol. 33, pp. 51~75(1995).

11. B.W. Spencer et al., "Results of MACE Tests M0 and M1," *Proc. of the 2nd OECD (NEA) CSNI Specialists Meeting on Molten Core Debris-Concrete Interaction*, KfK 5108, NEA/CSNI/R, pp. 357~372(1992).

12. M.T. Farmer et al., "MACE Core Coolability Test M1B," *20th Water Reactor Safety Meeting, Bethesda*, MD(1992).

13. Anthony. F. Mills, "*Heat Transfer*", Irwin(1992).

14. H. Alsmeyer et al., "Nuclear Science and Technology ; Molten corium/concrete interaction and corium coolability − A state of the art report − ", *Final Report, EUR16649EN*, European Commission(1995).

15. Suh, K.Y et al., "A Study on the Establishment of Severe Accident Experimental *Facility*", *Final Report, KAERI/RR-1636/95*, KAERI(1996).